

Utah State University

DigitalCommons@USU

Physics Capstone Projects

Physics Student Research

8-10-2018

Electron Yield Comparisons of Low and High-Density Polyethylene

Jordan Lee

Utah State University

Follow this and additional works at: https://digitalcommons.usu.edu/phys_capstoneproject



Part of the [Physics Commons](#)

Recommended Citation

Jordan Lee (with JR Dennison), "Electron Yield Comparisons of Low and High-Density Polyethylene," Senior Thesis, Utah State University, Logan, UT, August 2018.

This Article is brought to you for free and open access by the Physics Student Research at DigitalCommons@USU. It has been accepted for inclusion in Physics Capstone Projects by an authorized administrator of DigitalCommons@USU. For more information, please contact digitalcommons@usu.edu.



Physics 4900 Project

August 10, 2018

Electron Yield Comparisons of Low and High-Density Polyethylene

Jordan Lee

Justin Christensen and JR Dennison, Mentors

Physics Department of Utah State University

Introduction:

With continued growth of the aerospace industry and further reliance on its communication infrastructure, a general idea of environmental stresses and material feedback is needed. Terrestrial-based labs attempt to recreate certain conditions seen in orbit and beyond, in order to gauge how materials and equipment will react. The Electron Emissions Test (EET) Chamber, an apparatus of USU's Material Physics Group, is used to test certain characteristics of materials in space-like environments. This experiment attempted to discern electron yield characteristics of two molecularly similar polymers: Low-Density Polyethylene (LDPE) and High-Density Polyethylene (HDPE).

Materials:

Ethylene, the basis for these molecules, is a hydrocarbon. Alone, this hydrocarbon can be described as two carbon atoms double-bonded to each other with hydrogen atom bonding satisfying their valence requirements. This results in a coplanar molecule with prominent angular separations between the atoms. Polyethylene is an extension of this structure where the carbon atoms no longer form double bonds, but single bonds with each other. This allows for long threads of carbon with somewhat weak hydrogen bonding fulfilling valence requirements. Due to this alteration, the polymer can no longer stay in its coplanar orientation and is pushed into a staggered configuration.

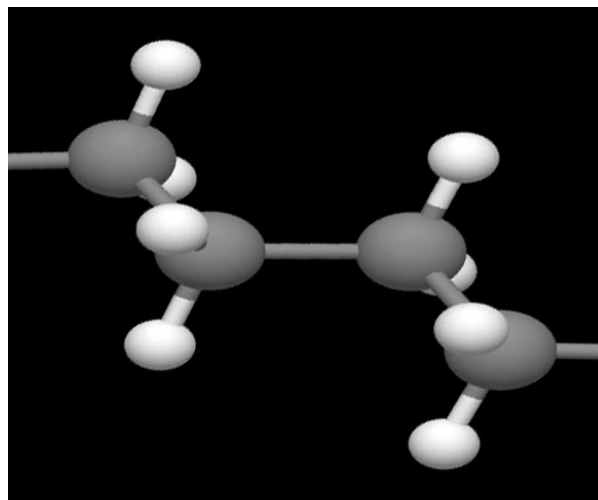
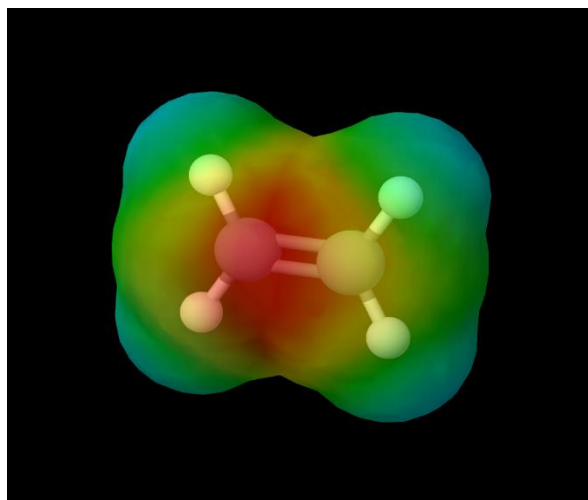


Figure 1 and 2: A representation of Ethylene and Polyethylene, respectively. Models generated from molview.org

Variations in branching and packing density help differentiate polyethylene structures. Extreme branching of carbon threads results in a less efficient packing configuration. In essence, certain characteristics of a polyethylene structure are directly influenced by how well the hydrocarbon structures can pack into a crystalline structure. Individual hydrocarbon chains rely heavily on the Van Der Waals force to clump together with other chains. If the branching reaches a certain threshold, packing efficiency is diminished and molecular density decreases. Low-Density Polyethylene ($0.910\text{--}0.940\text{ g/cm}^3$) is a good example of heavily branched hydrocarbon chains with decreased density. This polymer is used extensively in many industries due to its ease of creation and general chemical

resistance against acids, bases, and alcohols. Due to its poor packing, Low-Density Polyethylene (LDPE) is easily deformed at room temperature and has reduced ductile strength relative to other polyethylene structures. In structures where branching is minimal, packing approaches crystalline structures allowing for an increase in density. High-Density Polyethylene (0.941 g/cm^3) helps define this density and packing threshold. High-Density Polyethylene (HDPE) is also very common in many industries due to its chemical resistance. However, HDPE also exhibits more ductile strength and deformation resistance than LDPE. There are many other structures of polyethylene, but for the scope of this experiment only LDPE and HDPE were tested and compared.

Yield Overview:

The basis for electron yield measurement is dependent on the interaction of highly-energetic electrons with a material. These initial energetic electrons are considered primaries and within the scope of this experiment their energy and path is controlled. When the primaries reach a material they can exhibit varying behavior. Within the scope of this study only two behaviors are considered. The primary may interact with little degree and leave the material without much energy loss. Once this interaction occurs the electron is considered a backscattered electron. Emission energies of these backscattered electrons are, by convention, greater than 50 eV for energies above a 50 eV threshold. The other possibility is that the primary interacts with the material through continuous elastic and inelastic collisions. While the primary becomes embedded, the collisional energy is able to provide enough energy for electrons within the material itself to escape. Due to the potentials within the material, these emitted electrons are relatively lower in energy ($< 50 \text{ eV}$).

A model was derived, for metals, relating low-energy secondary emission distribution to the work function of the material itself (Chung and Everhart, 1974).

Experimental Setup:

The electron emission test chamber is used to contain the electron guns, sensors, and samples in a working pressure range of $1 * 10^{-7}$ to $5 * 10^{-9}$ Torr. These low pressures allow us to replicate the high to ultra-high vacuum environments seen in very high altitudes and space. These lower pressures help reduce the collisions of gas particles colliding with incoming beta particles used in the testing process.

The source of low energy electrons come from a gun referred to by its manufacturer (STAIB). The range of electron energies produced by this source is between 10 eV through 5 keV. Electron energies around 20 eV or below may have a higher degree of variance in their actual values. The source of high energy electrons come from a HEED gun, which is able to produce electrons of energies between 5 keV and 30 keV. Both are used in their respective testing, in order to have a broad range of yield testing.

The Hemispherical Grid Retarding Field Analyzer (HGRFA) is a sensor device that allows measurement of electron emission from materials undergoing electron bombardment (Wilson and Dennison, 2017).

Structurally it is a dome with a cavity below the surface. The first sensor, the collector, is a solid shell with a centered hole to allow for primary electrons to pass through. It is important that the incident electron beam is parallel to the surface normal of the material, because yield is dependent on angular resolution (Kite, 2006). The next shell underneath that is a wire mesh, the suppression grid, that allows the experimenters to apply a bias within the dome. This bias helps us differentiate between secondary and backscatter electrons. The final shell is another wire mesh, the inner grid, and allows us to match the sample potential and diminish any unwanted fields from influencing electron trajectories.

The process for a yield test is as follows:

TEY

Primary electrons are introduced by either the STAIB or HEED

The path of these primary electrons goes through the aperture of the HGRFA

The primary electrons impact with the sample surface and either embed to create secondary electrons or reflect without losing much energy (backscatter)

Both electron groups are captured by the HGRFA with no discrimination

BSEY

Primary electrons are introduced by either the STAIB or HEED'

The path of these primary electrons goes through the aperture of the HGRFA

The primary electrons impact with the sample surface and either embed to create secondary electrons or reflect without losing much energy (backscatter)

A -50 V bias, relative to the inner grid, is put onto the suppression grid to only allow higher energy backscatter electrons to reach the collector

In the case of insulators, such as polyethylene, precautions are taken to reduce charging. A low-energy electron flood gun assists in a reduction of positive charging on the surface. A UV LED (~290 nm) helps reduce negative charging (photoelectric effect) and some positive charging. In conjunction, these two devices help reduce surface charging of the material being tested (Thomson, 2005).

Analysis:

All data files contain headers and groupings of sensor data for a specific primary electron energy. Sensor data is kept in rows and of the values of volts. Given the constraints of the oscilloscope, each sensor collects 2500 data points for each pulse. Every pulse will yield 4 different sensor data lines with a total of 10000 points. Commonly there are 10 pulses per TEY and BSEY tests for every electron energy. A typical STAIB session with 23 energy levels can yield over two million data points. Retesting sample yield at certain energy levels is also done when necessary. This is done in order to correct for extreme outliers in a given dataset or to account for user error in the retrieving of the first data set.

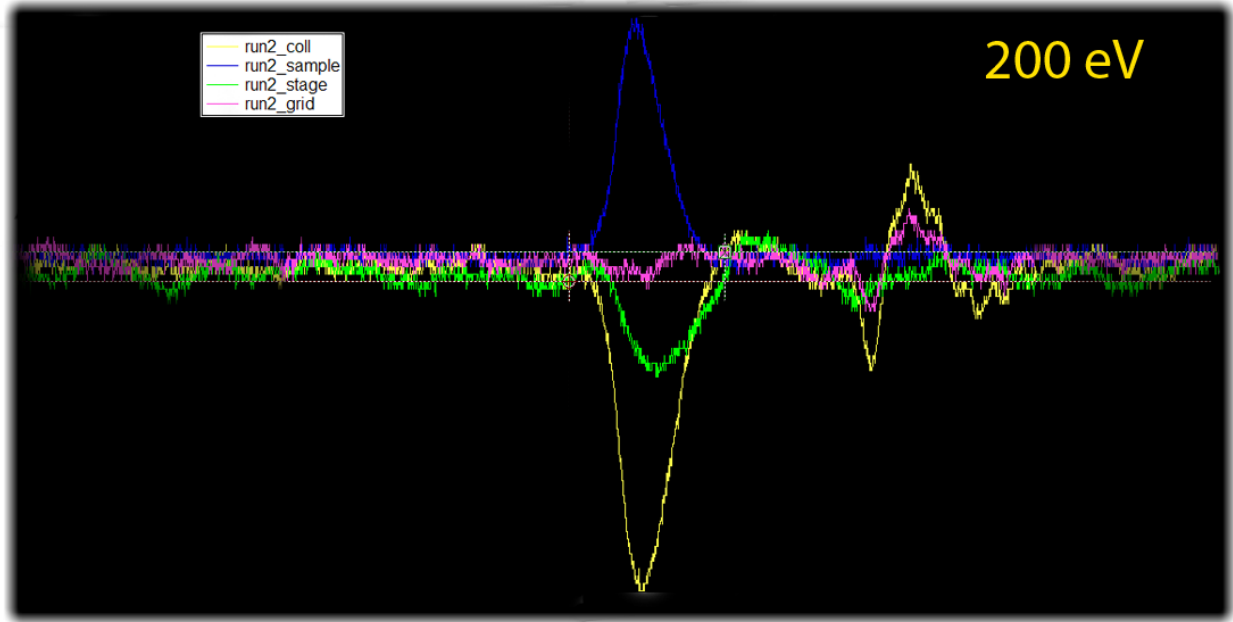


Figure 3: An example of signals collected at 200 eV during testing

In order to reduce uncertainty, only a subset of the data points is considered for analysis of yield. These points contain the prominence of the signal. To account for background noise in the signal, portions of the baseline signal are fitted to a sine or average function and removed from the main yield proportion signal. The values within the necessary ranges are summed and submitted to the yield equations shown below. This analysis was made possible by a script developed for the Igor Pro software, by Justin Christensen.

$$(TEY) \sigma = \frac{Q_{emit}}{Q_{incident}} = \frac{\int [I_{collector} + I_{grid} + I_{stage}] dt}{\int [I_{sample} + I_{collector} + I_{grid} + I_{stage}] dt}$$

$$(BSEY) \eta = \frac{Q_{emit}}{Q_{incident}} = \frac{C \int I_{collector} dt}{\int [I_{sample} + I_{collector} + I_{grid} + I_{stage}] dt}$$

$$(SEY) \delta = \sigma - \eta$$

Results Clarification:

Areas of interest for electron yield graphs are the two points in which yield crosses over unity and the peak yield energy range. The two unity transit areas are referred to as crossover energies. These areas characterize the energy at which incident and emitted electron ratios are equivalent. In those areas you would expect to have the least amount of charging of your sample, when bombarded with electrons of the required energy. The latter area of interest, peak yield energy range, characterizes the point in which the yield ratio is at its maximum. The material submitted to this energy range would charge positively at its fastest.

Due to the broad nature of the field, there are many models for fitting the yield data. For the scope of this report, a model augmented from Chung-Everheart was used (Christensen, 2017). While the model still requires relational anchors to material properties, it is still useful for interpreting areas of interest and the values therein.

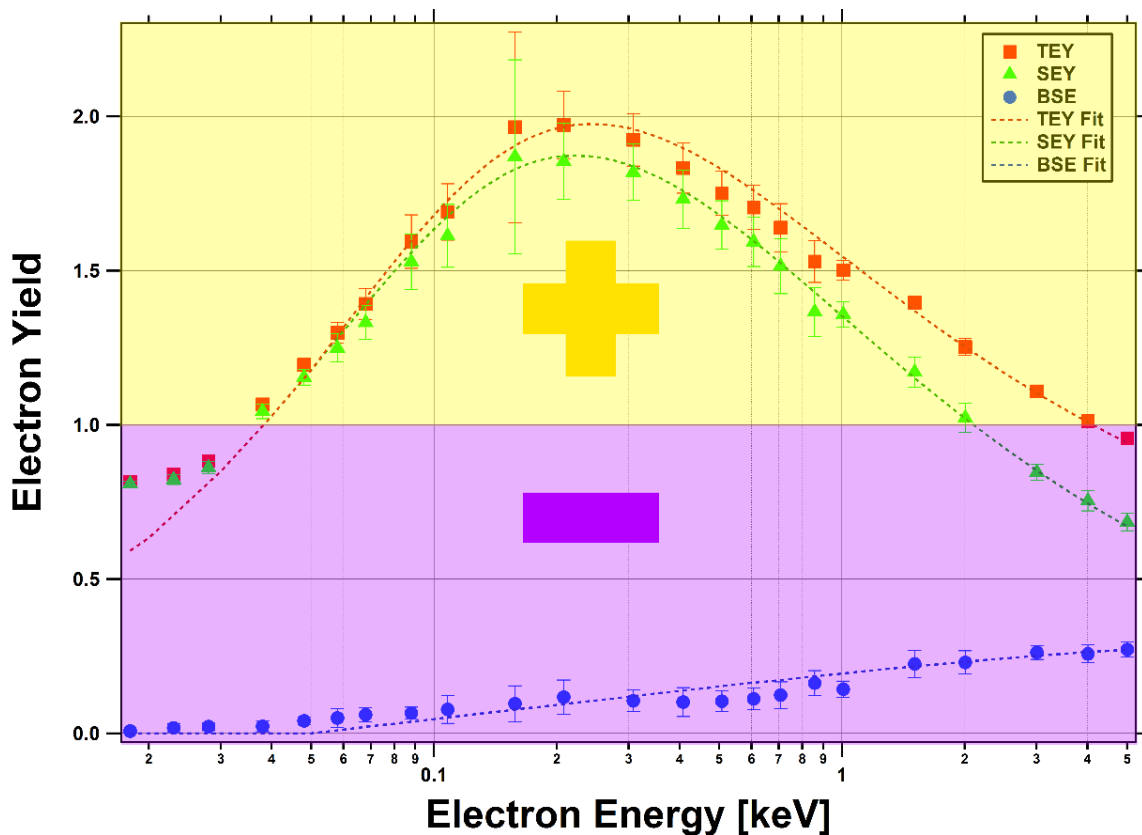


Figure 4: Electron yield curve of Tungsten with shading showing positive and negative material charging regimes

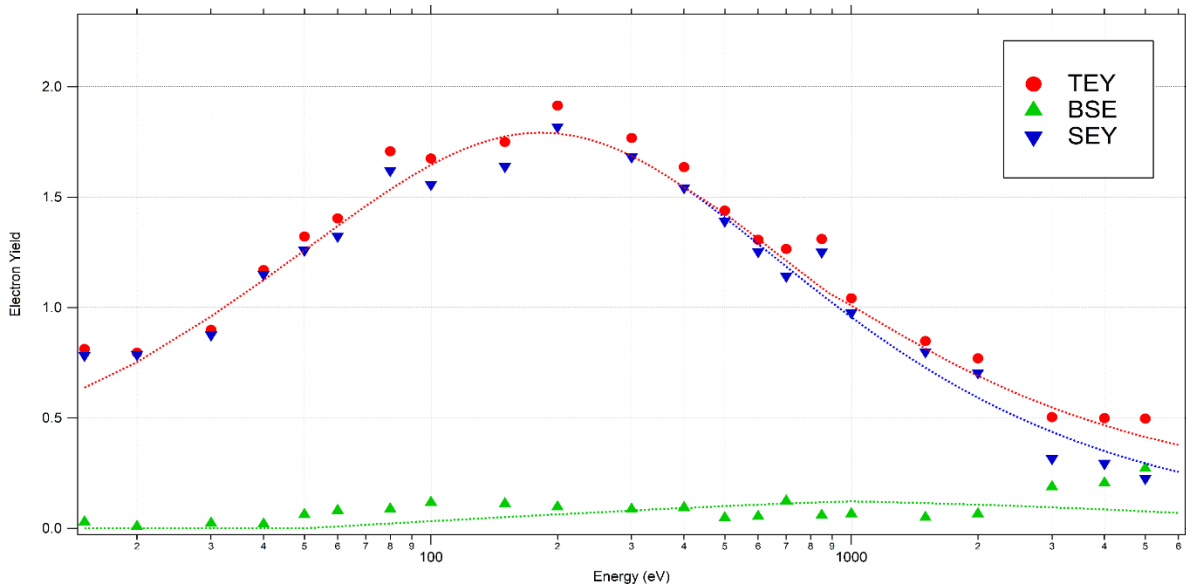


Figure 5: Electron yield curve of LDPE with TEY, SEY, and BSEY data points and fits

LDPE Results:

Even though precautions had been taken to alleviate surface charging, sometimes charging cannot be avoided. This is apparent in the data points situated between 80 eV to 200 eV and possibly between 3 keV to 5 keV. For the former range, the yield trends start to approach unity. This is due to the sample charging positively and attracting secondary electrons that would have otherwise escaped into the sensors. Regardless of this slight charging issue, the model provides insight into the crossover regimes and the peak yield location. The first crossover energy is situated at 32 ± 5 eV and the second crossover energy is situated at 1000 ± 5 eV. The data shows a peak yield of 1.8 ± 0.2 situated in a possible area between 150 eV to 200 eV.

HDPE Results:

The values of HDPE were similar to those seen in LDPE. The data showed a peak yield of 1.7 ± 0.1 situated at the same 150 eV to 200 eV range seen in LDPE. The first crossover energy was higher than LDPE, at 70 ± 5 eV. The second crossover energy was found to be at 1000 ± 5 eV. Charging was also very apparent in the higher energy regimes of the data testing. This is apparent in the figure shown below, in which the data exhibits a “V” shape towards the far right of the graph at around 2 keV. Similar to LDPE, the higher energy datasets will need to be retested in such a way that charging is absolutely accounted for.

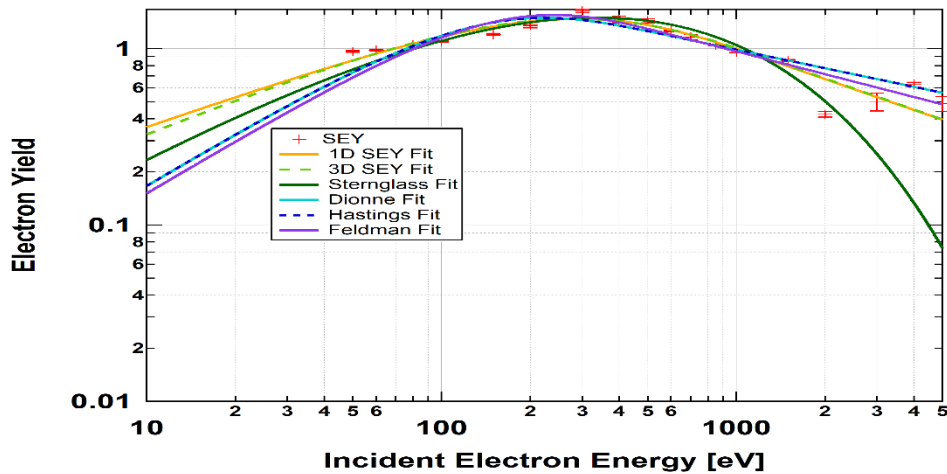


Figure 6: HDPE electron yield curve showing SEY data points and a multitude of fits used in electron yield research

Conclusion:

Considering the resolution of data collection and possible error introduced due to charging, it is not easy to discern variations between the two polyethylene datasets. The two materials may inherently be similar in the scope of electron yield, at least for experiments in which temperature is not accounted for. Historically, the Material Physics Group has been able to perform radiation induced conductivity measurements while manipulating sample temperature (Gillespie, 2013). The yield curves may vary drastically if temperature was controlled for these materials during yield testing. A possible explanation being that packing efficiency is reduced in LDPE due to its web-like and chaotic structure. The topology of the materials may change drastically when submitted to colder temperatures during testing. This topology could play an important role in the mechanics of electron yield. Further testing could include other forms of polyethylene such as cross-linked polyethylene (XLPE), linear low-density polyethylene (LLDPE), and very low-density polyethylene (VLDPE). Better resolution and further testing of polyethylene in its various structures and densities could provide insight into mechanics that influence electron yield.

References

Christensen, Justin, "Electron Yield Measurements of High-Yield, Low-Conductivity Dielectric Materials" (2017). *All Graduate Theses and Dissertations*. 6694.

Chung, M., and T. Everhart, 1974, "Simple Calculation of Energy Distribution of Low Energy Secondary Electrons Emitted from Metals under Electron Bombardment, " *J. Appl. Phys.* **45**,707

Kite, Jason T., "Secondary Electron Production and Transport Mechanisms By Measurement of Angle-Energy Resolved Cross Sections of Secondary and Backscattered Electron Emission from Gold" (2006). *All Graduate Theses and Dissertations*. 2089.

Gillespie, Jodie Corbridge, "Measurement of The Temperature Dependence of Radiation Induced Conductivity in Polymeric Dielectrics" (2013). *All Graduate Theses and Dissertations*. 1953.

Greg Wilson and JR Dennison, "Hemispherical Grid Retarding Field Analyzer Redesign for Secondary Electron Emission Studies," *Proceedings of the Utah NASA Space Grant Consortium Research Symposium*, May 8, 2017, Weber State University, Ogden, UT, 9 pp.

Thomson, Clint D., "Measurements of the Secondary Electron Emission Properties of Insulators" (2005). *All Graduate Theses and Dissertations*. 2093.